Reconstruction Algorithm for Probabilistic Inspection of Damage (RAPID) in Composites

Morteza TABATABAEIPOUR, Jan HETTLER, Steven DELRUE,
Koen VAN DEN ABEELE
Wave Propagation and Signal Processing Group, KU LEUVEN kulak, Kortrijk, Belgium,
Phone: +32(0)472107408, e-mail: morteza.tabatabaeipour@kuleuven-kulak.be

Abstract
Carbon-fiber-reinforced composites (CFRP) have become one of the most important structural materials in the last two decades. It is extensively used especially in the automotive and aerospace industry. Together with their popularity, important questions arise about their damage resistance and potential damage monitoring techniques. Reconstruction Algorithm for the Probabilistic Inspection of Damage (RAPID) tomography is a relatively fast method capable to provide information about the presence of damage, as well as about the damage location. The method uses the signal difference coefficient (SDC) value to describe the probability of the damage presence between the various transmitter-receiver pairs in an ultrasonic sparse array. The combination of SDC with a priori spatial probability distribution finally allows one to construct the tomographic image. The method can be applied both for linear defects, using a reference set of signals, or for non-linear signals by evaluating the sparse array signal matrix at different amplitudes. We will illustrate the methodology using experimental and numerical results of RAPID on an impacted and delaminated CFRP plates instrumented with sparse arrays up to 16 elements.

Keywords: Reconstruction Algorithm for the Probabilistic Inspection of Damage (RAPID), guided wave tomography, sparse array, Carbon-Fiber-Reinforced Composite (CFRP), ultrasound

1. Introduction

Nowadays, CFRP has already found its way to numerous areas of the industrial design and manufacturing. Thanks to an excellent weight-to-strength ratio, it's gradually becoming one of the key materials in many applications, ranging from automotive components to aerospace structural parts. On the other hand, the excellent strength-to-weight and stiffness-to-weight ratios of the CFRP are balanced with complicated post-damage behavior and the fact that CFRPs are difficult to repair. Nonetheless, parts of ever increasing dimensions and more complex shapes are being produced. This fact, together with the overall number of composite parts being used on a daily basis, calls for novel fast and more effective NDT and SHM methods.

Ultrasonic guided wave tomography (GWT) is a suitable candidate that meets the previously mentioned requirements. It is capable to interrogate large areas with limited number of transducers in very short time period. The current paper focuses on a damage visualization tool, based on Lamb wave inspection: Reconstruction Algorithm for the Probabilistic Inspection of Damage (RAPID). Unlike classic ultrasonic methods that use Time-of-Flight (TOF) or attenuation, the center point of the RAPID method is the Signal Difference Coefficient (SDC). SDC describes the dissimilarity of two signals acquired in two states, generally in the intact and damage state. By using the signals from sparse array and corresponding SDC values, we are able to calculate the damage presence probability in the inspected area. RAPID was described in detail by Gao et al. [1, 2, 3]. Further improvements of the method were made by Sheen et al. [4]. So far, most of the experimental work was done on rather simple aluminium plate-like structures.

In this paper, we will show that the RAPID technique is able to localize delaminations and impact damage in CFRP plate structures. In addition, we will demonstrate, with numerical simulations as well as with experimental data, that it can be used for baseline-free nonlinear tomographic inspection of simple CFRP plate structures.

2. Methods

RAPID utilizes Lamb wave propagation data between transmitter-receiver pairs acquired from an ultrasonic sparse array that is coupled to the interrogated structure. In general, matrix data are acquired for two different experimental conditions (in our case: either before & after damage, or at low and high excitation amplitude). Based on the different acquisitions, signal difference coefficient values (SDC) can be calculated. As presented in literature, several options have been proposed how to calculate SDC value for a given transducer-receiver pair. In the presented work, we used the SDC value based on the correlation coefficient or Mean Square Error (MSE) formula.

Let the signal between the transducer i and receiver j in the sparse array be denoted as B_{ij} for the case of the intact (baseline) state and D_{ij} for the damaged state. Then the correlation SDC value can be calculated as:

$$\rho_{ij} = \frac{Cov\left(B_{ij}(t),D_{ij}(t)\right)}{\sigma\left(B_{ij}(t)\right)\sigma\left(D_{ij}(t)\right)} = \frac{\sum_k^N\left(B_{ij}(t_k)-\mu_{B_{ij}}\right)\left(D_{ij}(t_k)-\mu_{D_{ij}}\right)}{\sqrt{\sum_k^N\left(B_{ij}(t_k)-\mu_{B_{ij}}\right)^2}\sqrt{\sum_k^N\left(D_{ij}(t_k)-\mu_{D_{ij}}\right)^2}} \quad (1)$$

$$SDC_{ij} = 1 - \rho_{ij}\,, \quad (2)$$

where ρ_{ij} stands for the correlation coefficient, t_k is the sampled time, N is the total number of the transducers in the sparse array and Cov and σ are the covariance and standard deviation operations. Alternatively, the formula for MSE SDC value can be calculated as follows:

$$SDC_{ij} = \frac{1}{N}\sum_k^N\left(B_{ij}(t_k) - D_{ij}(t_k)\right)^2 \quad (3)$$

Both SDC expressions describe the dissimilarity between the two signals and therefore it is also a measure of the damage presence probability in the area between transmitter i and receiver j. In order to extrapolate the sole SDC value to the area along the direct propagation path between the transmitter and receiver; we define the a priori spatial probability distribution $s_{ij}(x,y)$ as follows:

$$\begin{cases} s_{ij}(x,y) = \frac{\beta - R_{ij}(x,y)}{1-\beta} & for\ \beta > R_{ij}(x,y) \\ s_{ij}(x,y) = 0 & for\ \beta \le R_{ij}(x,y)\,, \end{cases} \quad (4)$$

where β is the shape parameter, (x,y) the coordinates of the mesh point and

$$R_{ij}(x,y) = \frac{\sqrt{(x_i-x)^2+(y_i-y)^2}+\sqrt{(x_j-x)^2+(y_j-y)^2}}{\sqrt{(x_j-x_i)^2+(y_j-y_i)^2}} \quad (5)$$

is the ratio of the sum of distances from transmitter and receiver to point (x, y) to the distance between the transmitter and receiver. The typical shape of the spatial distribution s_{ij} is depicted in Figure 1.

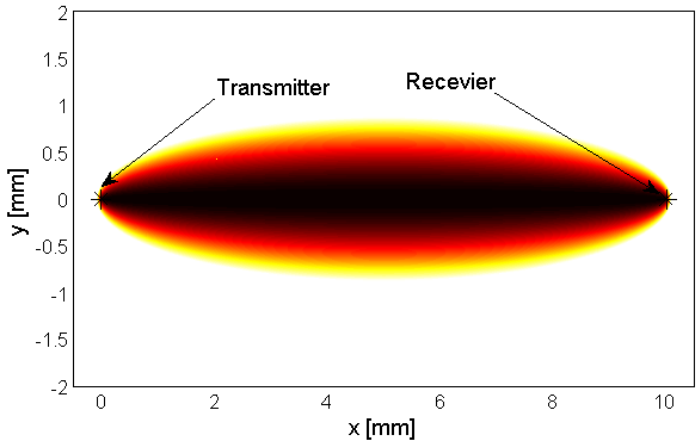

Figure 1. Spatial probability distribution s_{ij} for given value of parameter β

To obtain the final damage presence probability map, we multiply the SDC_{ij} value with the appropriate distribution $s_{ij}(x, y)$ for all the transducer-receiver pairs. As a last step in the tomographic procedure, the partial contributions have to be summed together. Applying these steps, we obtain the final formula for the damage presence probability:

$$P(x, y) = \sum_{i=1}^{N} \sum_{j=1, j \neq i}^{N} SDC_{ij} s_{ij} \,, \tag{6}$$

where N is the total number of transducers in the sparse array.

In most cases the baseline signals correspond to the intact free condition, whereas the second set of measurements is performed on a damaged sample. Alternatively, amplitude dependent measurements can be performed on a sample in the same damage state, eliminating the need for baseline corrections due to varying experimental conditions. As such, one can utilize the scaling-subtraction processing in order to use RAPID to localize defects without the knowledge of the intact baseline [5]. In this case, the baseline signal is substituted by a measurement at low amplitude excitation on the damaged sample. The response to a high amplitude excitation signal comprises the second set of signals, and needs to be compared to an up-scaled version of the low amplitude response by applying a scaling factor

$$a = \frac{D}{B}, \tag{7}$$

where D and B are the high and low excitation amplitudes respectively, leading to an SDC coefficient that is calculated with the adapted MSD algorithm as follows:

$$SDC_{ij} = \frac{1}{N} \sum_{k}^{N} \left(aB_{ij}(t_k) - D_{ij}(t_k) \right)^2 \tag{8}$$

If the system is purely linear, noiseless and exhibits no nonlinear behaviour, the SDC_{ij} value calculated using eq.(8) is *0*. However, if there is a source of non-linearity, possibly induced by a delamination or an impact damage, the SDC values may change for specific transmitter-receiver pairs. This effect then allows us again to apply the same RAPID tomographic methodology to localize the possible sources of nonlinearity.

3. Numerical simulations

Numerical simulation were carried out in order to ascertain the feasibility of the linear and nonlinear defects detection in thin CFRP plates using the RAPID method. COMSOL Multiphysics® FEM software suite was used to model both linear and nonlinear delamination. In accordance with the experiments, the sample was modelled as an orthotropic plate with dimensions of 288 x 296 x 2.7 mm with damping. The simulated sparse array consisted of 8 transducers that were modelled as rectangular patches. The elastic properties of the simulated plate are noted in Table 1. 20 cycled hanning windowed tone bursts were used to excite the plate and 2000 points were collected at the receiving positions.

Table 1. Elastic properties of the simulated CFRP plate

Young's modulus [GPa]	Shear modulus [GPa]	Poisson's ratio
E_{xx} = 127.11	G_{xy} = 5.0	ν_{xy}=0.320
E_{yy} = 8.34	G_{yz} = 2.7	ν_{yz}=0.461
E_{zz} = 8.85	G_{zx} = 4.8	ν_{zx}=0.009

3.1 Linear delamination

The linear delamination in the plate was modelled as a block-shaped subdomain with dimensions of 20 x 20 mm. The delamination was located in ¼ of the total thickness of the plate. The elastic properties of this subdomain were modelled to be only 90% of the elastic properties of the maternal material given in Table 1.

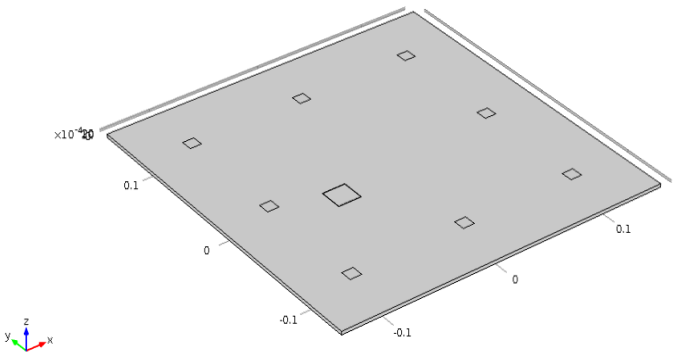

Figure 2. Simulated CFRP plate with delamination

3.2 Nonlinear delamination

The nonlinear delamination was simulated using the spring-damper model proposed earlier by Delrue and Van Den Abeele in [6]. Using this model, the delamination exhibits an amplitude dependent nonlinear 'clapping' behavior, generating both harmonics and subharmonics of the excitation frequency. The scheme of this model can be seen in Figure 3.

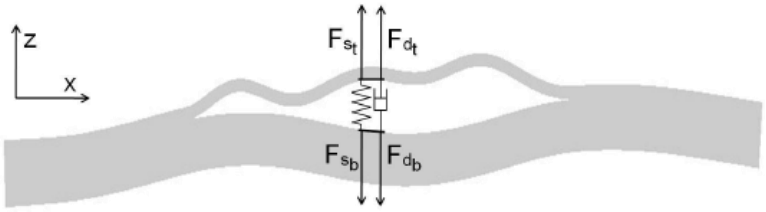

Figure 3. Spring-damper model of the nonlinear delamination

4. Results

4.1 Numerical simulations

Figure 4 to 6 show the results of the simulated scenarios. Different combinations of linear and nonlinear defects were tested and the results were evaluated.

At first, a simulated linear defect was analyzed by the linear and nonlinear RAPID methodology. Figure 4 clearly shows that the linear RAPID procedure (using intact condition baseline signals) can localize the linear defect. However, as shown in Figure 5, the identification of a linear defect is not possible using the NL RAPID approach, due to the fact that linear defects do not induce amplitude dependent behavior.

Conversely, a simulated nonlinear defect was clearly localized using the NL RAPID methodology (see Figure 6) and not by its linear version (not shown).

The obtained tomographic images confirm that the NL RAPID is a promising tool to recognize and localize incipient defects for which the reduction of the linear elasticity parameters may be too small to be detected by a linear reconstruction tool.

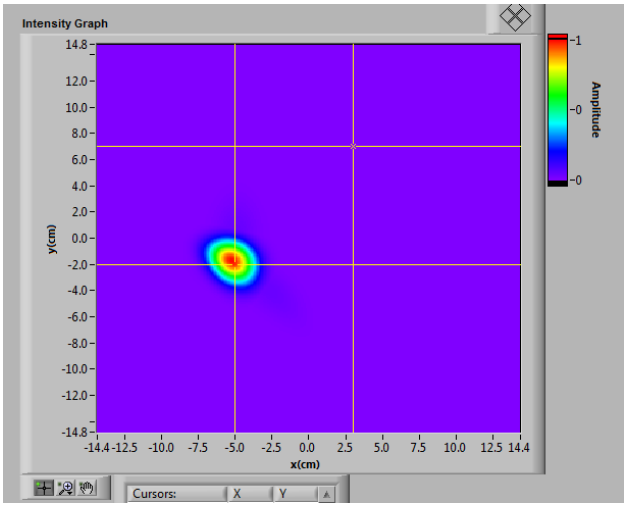

Figure 4. Image obtained by linear RAPID on a sample with a linear delamination, actual location of damage is (-5, -2)

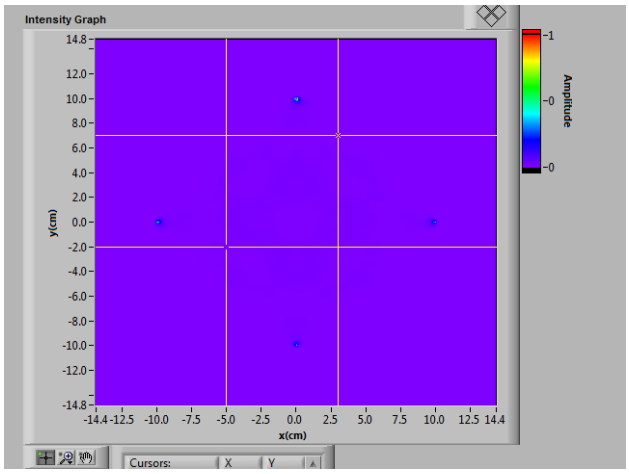

Figure 5. Image obtained by linear RAPID on a sample with a nonlinear delamination, actual location of damage is (-5, -2)

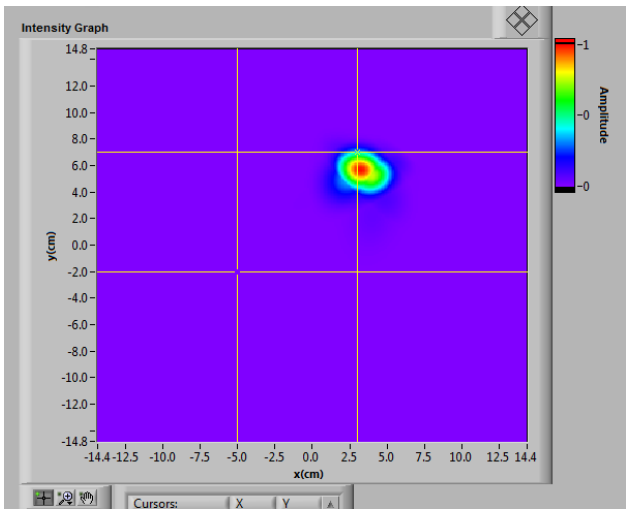

Figure 6. Image obtained by NL RAPID on a sample with a nonlinear delamination is actual location of damage is (3, 7)

4.2 Experimental results

Actual Lamb wave propagation measurements on two different samples were conducted in order to verify the performance of the proposed nonlinear RAPID tomographic reconstruction process. The testing specimen was a CFRP plate with dimensions 500 x 500 mm. The thickness is 8 mm and there are 10 layers. The orientation of the plies results in quasi-isotropic elastic properties of the plate. The specimen was instrumented with 16 piezo composite PI patches oriented in a rectangular manner around the edges of the sample.

All transducers were subsequently excited one by one with a 3-cycle hanning windowed sine burst, while the signals from the rest of the array were digitized by the NI PXI-5422 high speed digitizers. The conventional C-scan carried out on the impacted sample is depicted in Figure 7. There is a clearly visible indication of the damaged (impacted) area in the upper right quadrant. The result of the tomographic reconstruction obtained by inspecting the same sample using the linear RAPID methodology can be seen in Figure 8.

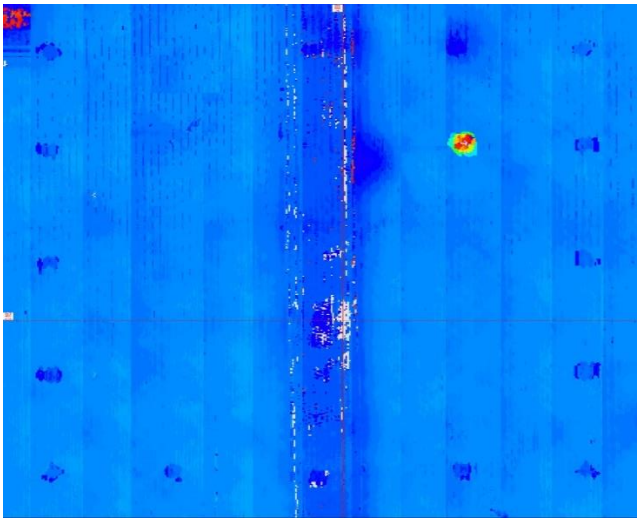

Figure 7. C-scan of the impacted CFRP sample, red area indicates the impact zone

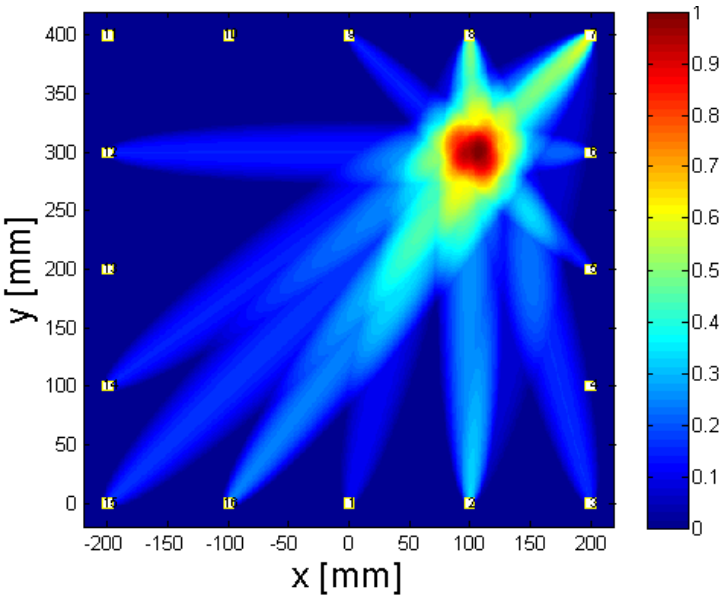

Figure 8. Image obtained by Linear RAPID, rectangular pattern yellow squares around the image indicate the transducers positions on the sample

5. Conclusions

Simulated and empirical data of Lamb wave propagation in damaged composites were evaluated using the linear and nonlinear RAPID methodology, giving rise to damage reconstruction maps. The linear RAPID method was successfully employed to identify and localize linear defects either using simulated or experimental data. However, it was shown that the linear RAPID tool is not practical to examine nonlinear defects. Conversely, as shown by numerical data, only the Nonlinear RAPID methodology can be efficiently employed in the detection of a nonlinear delamination. Further work will focus on the confirmation of the NL RAPID methodology using experimental data.

Acknowledgements

The research leading to these results has gratefully received funding from the European Union Seventh Framework Programme (FP7/2007- 2013) under Grant Agreements n° 284562 (Saristu) and n [3]° 314768 (ALAMSA).

References

[1] H Gao, Y Shi, J L Rose, " Guided wave tomography on an aircraft wing with leave in place sensors," *Review of Quantitative Nondestructive Evaluation,* vol. 24, pp. 1788–1795, 2005.

[2] X Zhao, H Gao, G Zhang, B Ayhan, F Yan, C Kwan, J L Rose, "Active health monitoring of an aircraft wing with embedded piezoelectric sensor/actuator network: I. Defect detection, localization and growth monitoring," *Smart Materials and Structures,* vol. 16, no. 4, pp. 1208-1217, 2007.

[3] T R Hay, R L Royer, H Gao, X Zhao, J L Rose, "A comparison of embedded sensor Lamb wave ultrasonic tomography approaches for material loss detection," *Smart Materials and Structures,* vol. 15, no. 4, pp. 946–951, 2006.

[4] B Sheen, Y Cho, "A study on quantitative lamb wave tomogram via modified RAPID algorithm with shape factor optimization," *International Journal of Precision Engineering and Manufacturing*, vol. 13, no. 5, pp. 671–677, 2012.

[5] M Scalerandi, A S Gliozzi, B E Anderson, M Griffa, P A Johnson, T J Ulrich, "Selective source reduction to identify masked sources using time reversal acoustics," *Journal of Physics D: Applied Physics,* vol. 41, 155504, 2008.

[6] S Delrue, K Van Den Abeele, "Three-dimensional finite element simulation of closed delaminations in composite materials," *Ultrasonics,* vol. 52, no. 2, pp. 315-332, 2012.